Electronic Supporting Information (ESI)

Rational Design of Hyperbranched 3D heteroarrays of SrS/CdS: Synthesis, Characterization and Evaluation of photocatalytic Properties for Efficient Hydrogen Generation and Organic Dye Degradation

Ziyauddin Khan, Tridip Ranjan Chetia and Mohammad Qureshi*
Material Science Laboratory, Department of Chemistry, Indian Institute of Technology Guwahati, Assam-781039, India

Schematic illustration of photocatalytic hydrogen generation

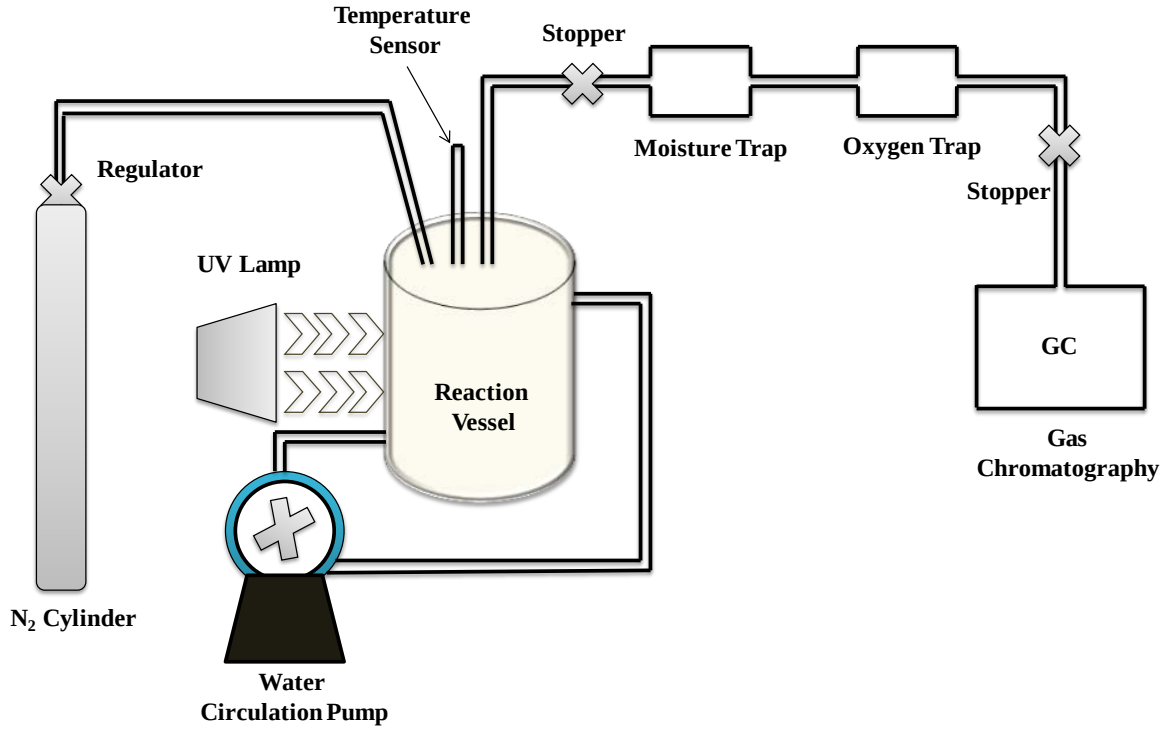

Figure S1. *Schematic presentation of photocatalytic water splitting system*

Mechanism of the formation of hyperbranched 3D SrS/CdS heteroarrays

In literature, it was reported that organic molecules played an important role for the formation of inorganic 3D architecture. For example, 3D CdS nanocrystals with flower-like structure were prepared using hexamethylenetetramine as the capping agent [1], 3D dendritic CdS nanoarchitectures were prepared using cetylpyridinium chloride as the capping agent [2] etc. However, previous studies showed that the hydroxyl groups could also involve stabilizing, order, and controlling the spatial arrangement of the inorganic nanoparticles by

spreading over the surface of these nanoparticles [3-6]. Interestingly, in the current study thioglycolic acid is involved in the preparation of hyperbranched 3D SrS/CdS heteroarrays as a sulfur precursor having hydroxyl group. Therefore, it is proposed that the hydroxyl group of thioglycolic acid might spread over the synthesized SrS and CdS nanoparticles. Amount of SrS NPs are less in the solution which leads to the ordered growth of CdS NWs on SrS NPs at hydrothermal condition, and further results in the formation of hyperbranched 3D SrS/CdS architecture. The detailed schematic of proposed mechanism for the formation of 3D SrS/CdS is discussed in scheme 1.

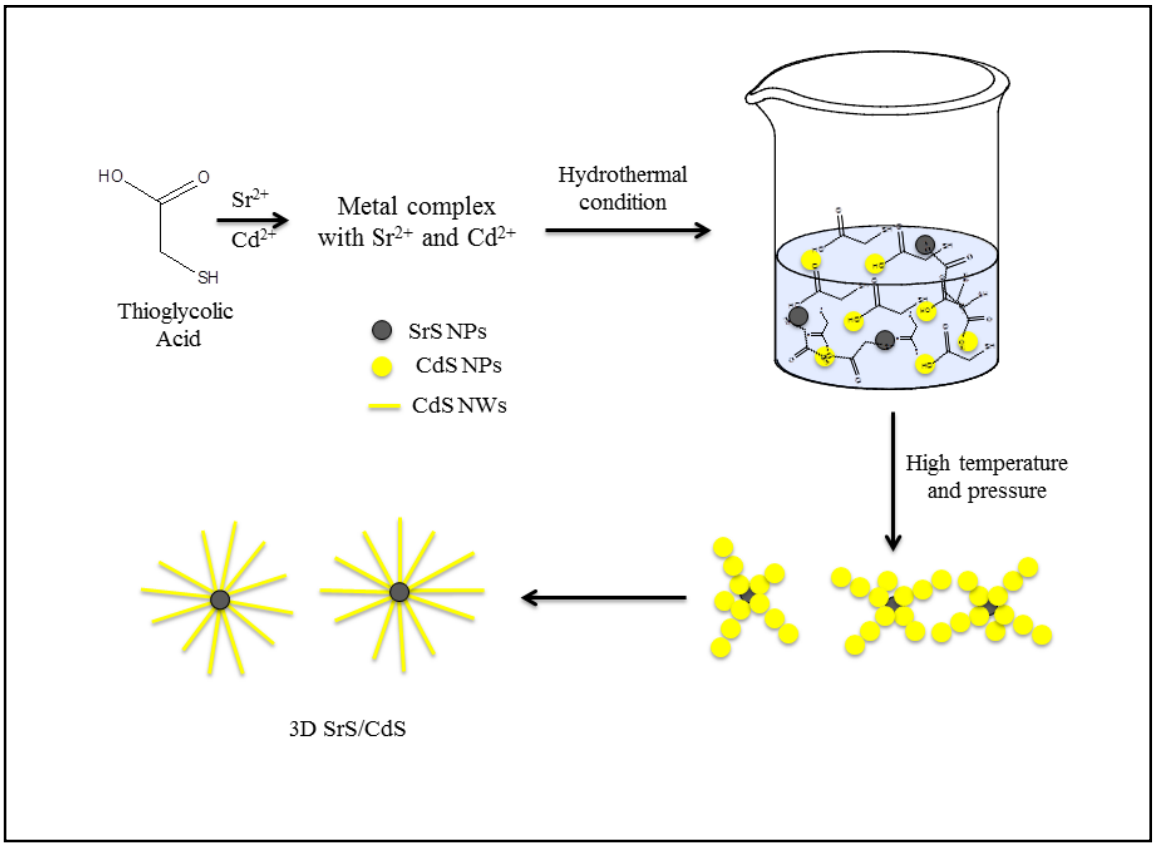

Scheme 1: Schematic illustrations of the formation of the hyperbranched 3D SrS/CdS heteroarrays

Transmission Electron Microscope images for 1D CdS NWs and SrS NPs

Illustrative TEM images for the prepared free standing 1D CdS NWs and SrS NPs were shown in Figure S2. TEM features shows that free standing 1D CdS NWs have diameters around 40-50 nm while SrS NPs have of 20 nm diameter.

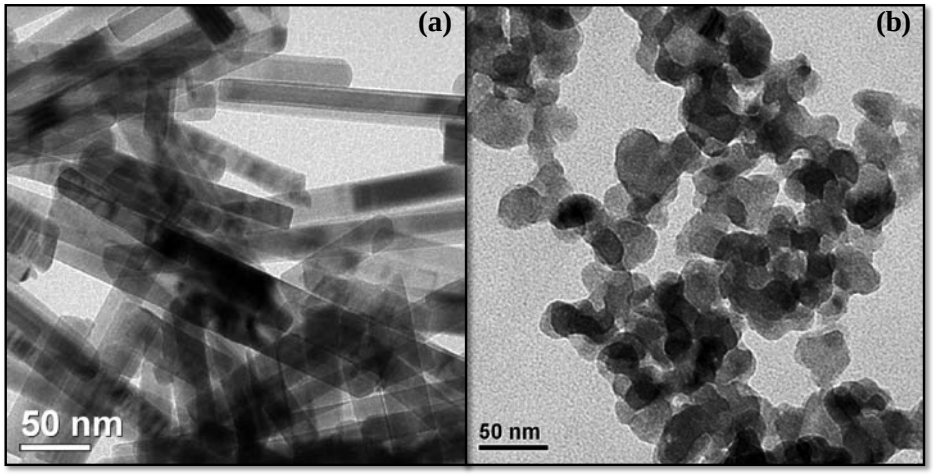

Figure S2. *Transmission Electron Microscope images of (a) free standing 1D CdS NWs and (b) SrS NPs.*

FE-SEM images of hyperbranched 3D SrS/CdS

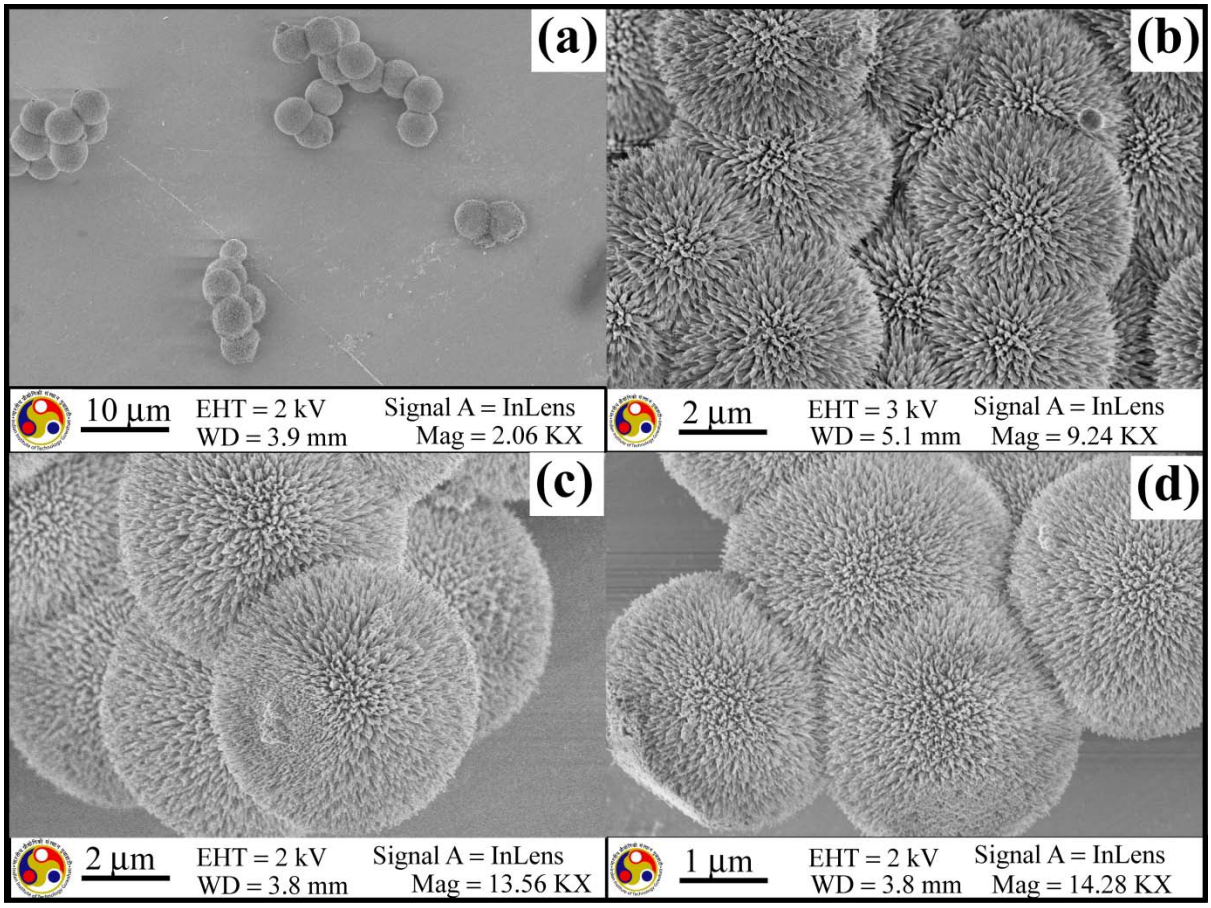

Figure S3. *FE-SEM images of Hyperbranched 3D SrS/CdS at different magnifications*

Low resolution Transmission Electron Microscope images for 3D SrS/CdS

At low magnifications the TEM images of the larger particles were not clear, partly due to the fact that electron beam is not able to transmit through and hence they appeared as the dark

patches (*shown in Figure S4*). Therefore, in order to obtain the clear structure of the particle TEM image was taken for the particle having smaller size (the sample was prepared from the supernatant of the SrS/CdS dispersion).

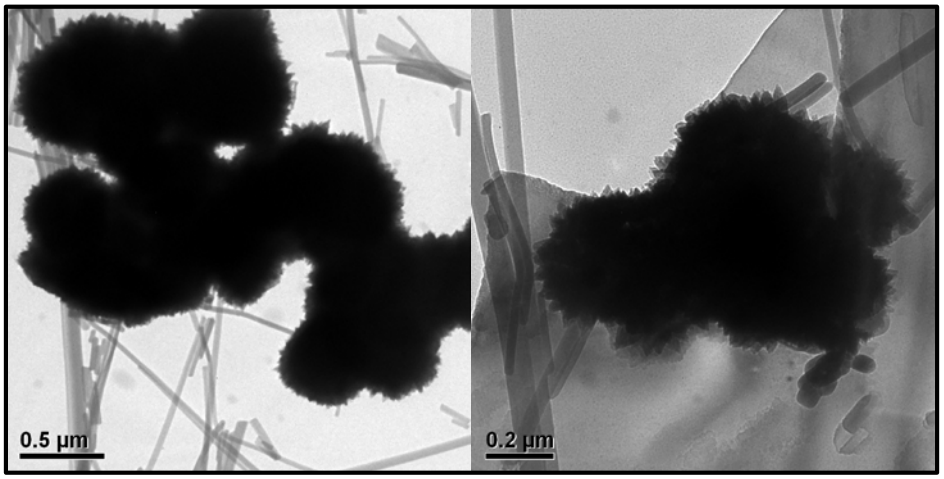

Figure S4. *Low resolution Transmission Electron Microscope images of 3D SrS/CdS. Particles are not very visible as they appeared as dark spots.*

Energy dispersive X-ray and selected area electron diffraction (SAED) pattern

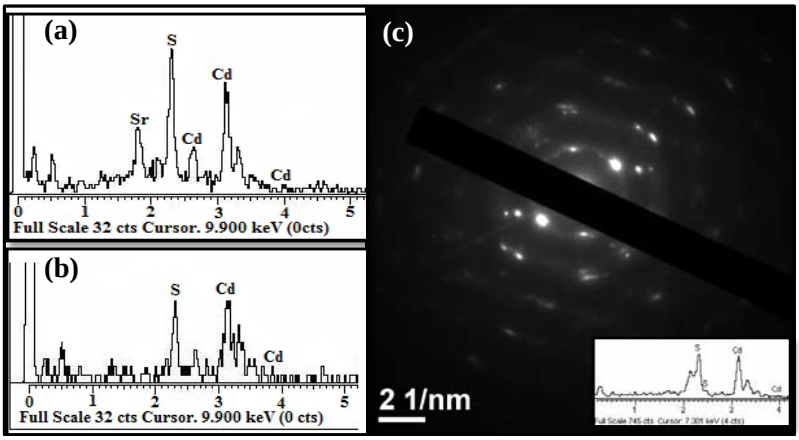

Figure S5. *Energy dispersive X-ray (EDX) pattern at (a) the center and (b) the edge of flower like 3D SrS/CdS (c) Selected Area Electron Diffraction (SAED) pattern of CdS NWs. From SAED it is clear that disrupt CdS NWs from 3D SrS/CdS are in hexagonal phase. Inset shows the EDX of that particular CdS NWs.*

Scanning Electron Microscope image of SrS/CdS at different ratios of Sr^{2+} and Cd^{2+}

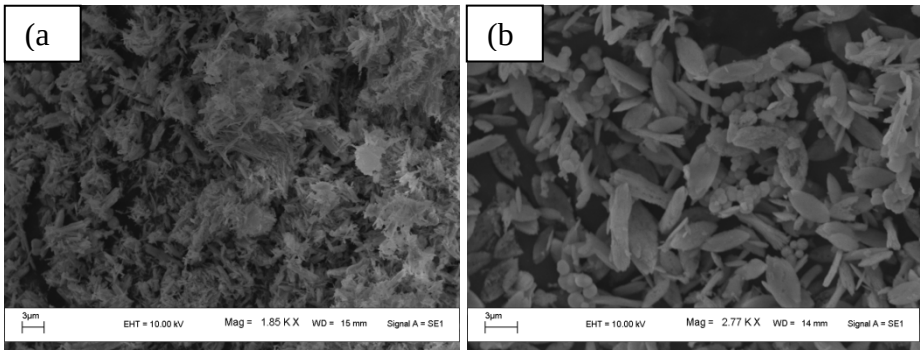

Figure S6. *SEM images of SrS/CdS at different ratios (a) Sr/Cd ratio is 1:1 (b) Sr/Cd ratio is 1:0.43. At different ratio of Sr and Cd no flower like structure was observed.*

Hydrogen production rate at different time by hyperbranched 3D SrS/CdS and 1D CdS NWs

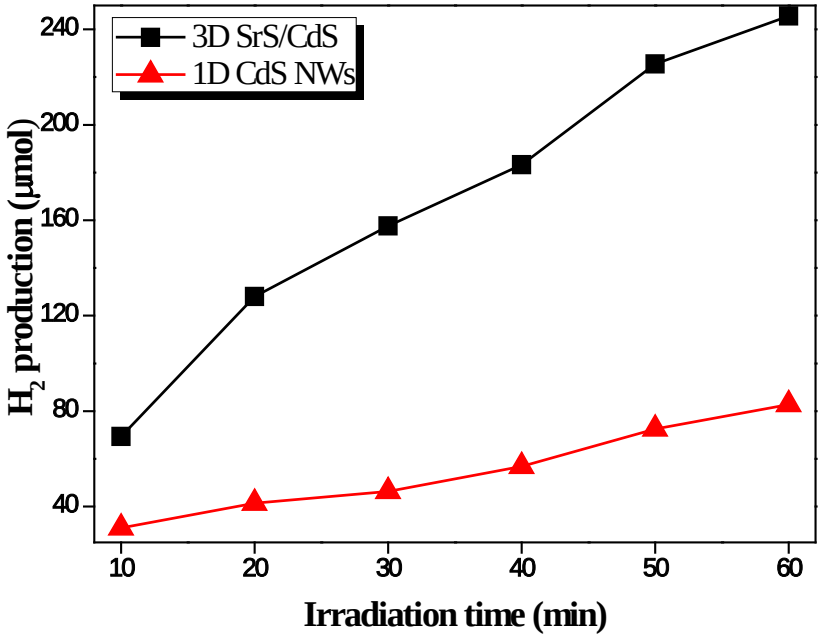

Figure S7*. Photocatalytic hydrogen production as a function of irradiation time for 1D CdS NWs and hyperbranched 3D SrS/CdS. 20 mg catalyst suspended in 50 mL aqueous solution containing* Na_2S *and* Na_2SO_3*. Hydrogen production given in the figure is in respect to 20 mg catalyst.*

Comparative AQY value of CdS based semiconductor

The comparative efficiencies of CdS based photocatalyst reported in literature with hyperbranched 3D SrS/CdS is shown in Table S1. From Table S1, it is clear that the present hyperbranched 3D SrS/CdS shows higher AQY than most of the previously reported CdS based photocatalysts.

Table S1. AQY values of CdS based photocatalysts for hydrogen generation under visible light irradiation

photocatalyst	synthetic method	co-catalyst	AQY* (%)	ref
$Mn_{1-x}Cd_xS$	hydrothermal	RuO	7	7
$Cd_{1-x}Zn_xS$ (x=0.2)	thermal sulfurization	-	10.23	7
Pt/CdS NWs	chemical deposition	-	3.9	7
CdS/ZnO	two step precipitation	Pt	3.2	8
SrS/CdS	precipitation	Pt	5.83	9
CdS/ZnS	H_2S thermal sulfurization	-	10.2	7
CdS/ ZTP	-	-	5.84	10
photocatalyst	**synthetic method**	**co-catalyst**	**AQY* (%)**	**ref**
CdS/Graphene	solvothermal	Pt	22.5 (420 nm)	11
CdS/MWCNT	hydrothermal	-	2.16 (420 nm)	12
$CdS/KNbO_3$	ion adsorption, precipitation	NiO	8.8	7
$Ni/NiO/KNbO_3/CdS$	-	-	4.4	13
CdS-ZnS	-	-	0.60	14
CdS/Ti-MCM-41	ion exchange, sulfurization	Pt	2.6	15
CdS	impregnation method	0.2 wt% MoS_2	7.3 (720 nm)	16, 17
3D SrS/CdS	hydrothermal	-	10	Present work

*The value of AQY varies with the evaluation method and the system of interest.

UV-Vis absorption spectra of Methyl Orange

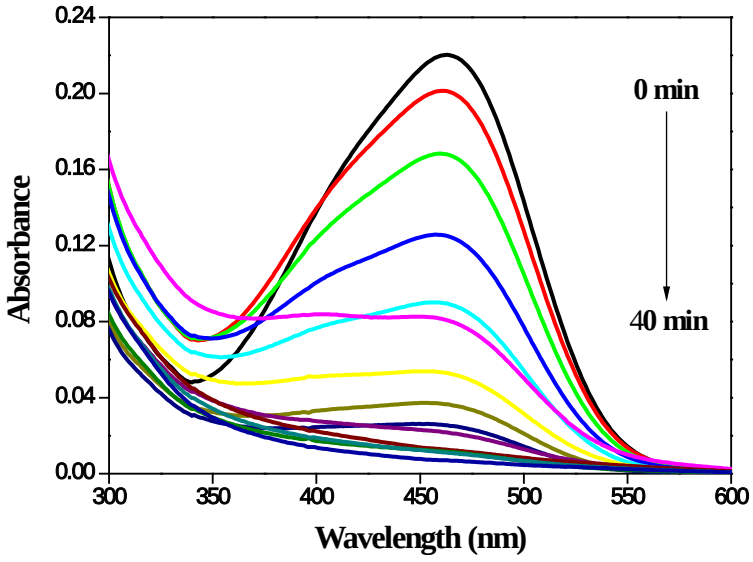

***Figure S8**. UV-Vis absorption of methyl orange in presence of 1D CdS NW photocatalyst*

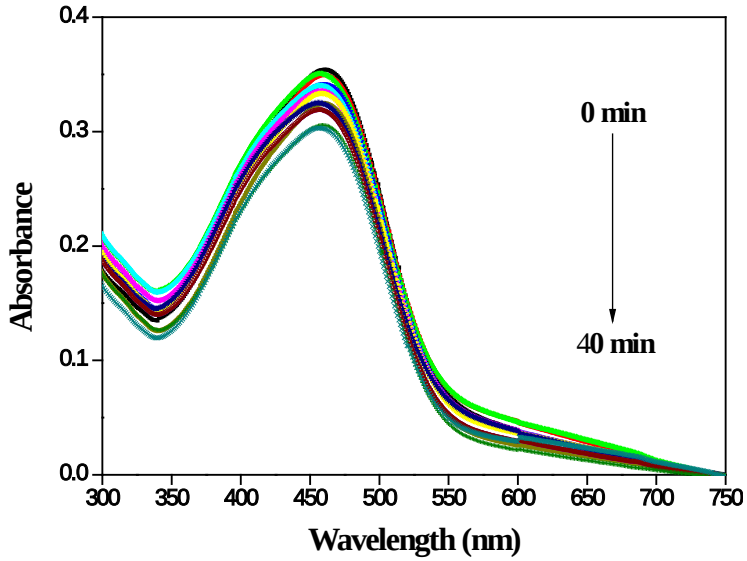

Figure S9. *UV-Vis absorption of methyl orange in presence of SrS NPs photocatalyst*

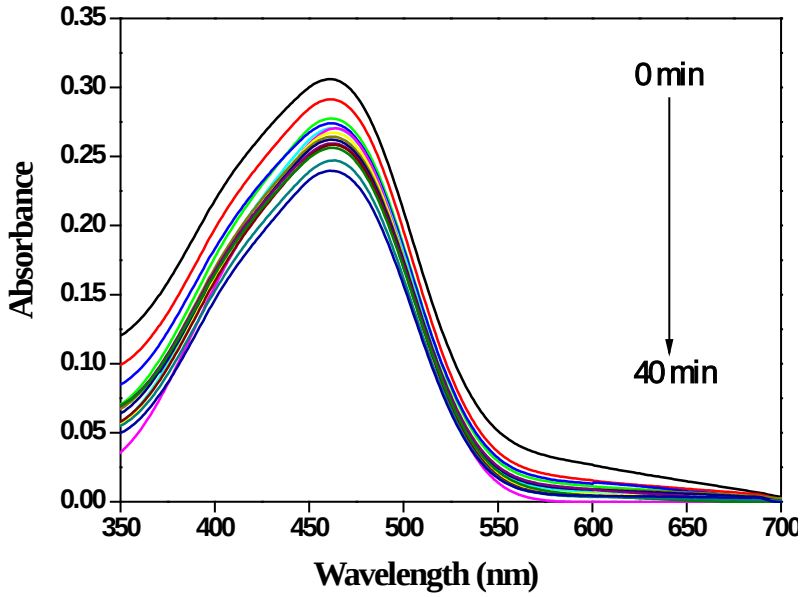

Figure S10. *UV-Vis absorption of methyl orange in presence of* Fe^{2+} *metal ion by hyperbranched 3D SrS/CdS*

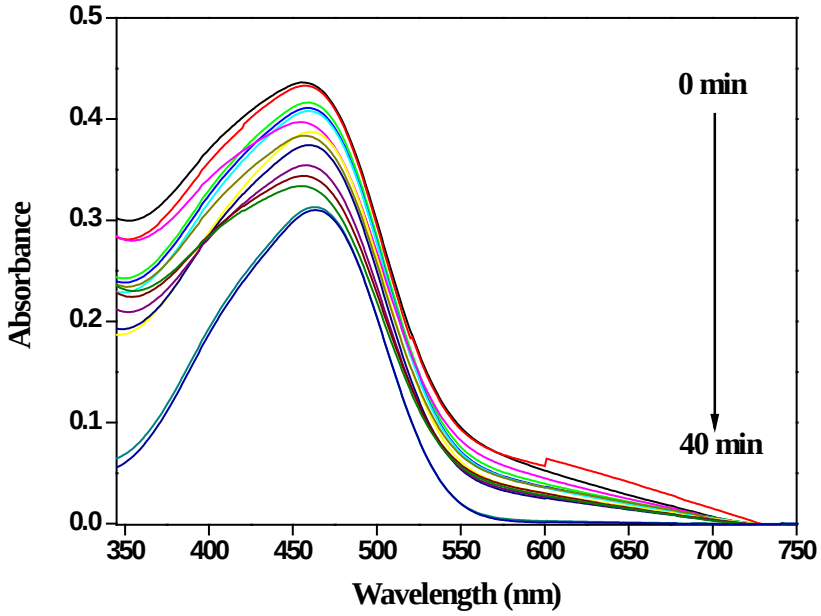

Figure S11. *UV-Vis absorption of methyl orange solution in deoxygenated water by hyperbranched 3D SrS/CdS*

References

1- F. Chen, R. Zhou, L. Yang, N. Liu, M. Wang and H. Chen, *J. Phys. Chem. C*, 2008, **112**, 1001.

2- D. Wang, D. Li, L. Guo, F. Fu, Z. Zhang and Q. Wei, *J. Phys. Chem. C*, 2009, **113**, 5984.

3- D. K. Bozanic, V. Djokovic, J. Blanusa, P. S. Nair, M. K. Georges and T. Radhakrishnan, *Eur. Phys. J. E*, 2007, **22**, 5.

4- G. Carrot, D. Rutot-Houze, A. Pottier, P. Degee, J. Hilborn and P. Dubois, *Macromolecules*, 2002, **35**, 8400.

5- P. Rodriguez, N. Munoz-Aguirre, E. S. Martinez, G. G. de la Cruz, S. A. Tomas and O. Z. Angel, *J. Cryst. Growth*, 2008, **310**, 160.

6- S.-W. Yeh, T.-L. Wu and K.-H. Wei, *Nanotechnology*, 2005, **16**, 683.

7- X. Chen, S. Shen, L. Guo and S. S. Mao, *Chem. Rev.*, 2010, **110**, 6503.

8- X. Wang, G. Liu, G. Q. Lu and H.-M. Cheng, *Int. J. Hydrogen Energ.*, 2010, **35**, 8199.

9- H. Liu, K. Zhang, D. Jing, G. Liu and L. Guo, *Int. J. Hydrogen Energ.*, 2010, **35**, 7080.

10- K. M. Parida, N. Biswal, D. P. Das and S. Martha, *Int. J. Hydrogen Energ.*, 2010, **35**, 5262.

11- Q. Li, B. Guo, J. Yu, J. Ran, B. Zhang, H. Yan and J. R. Gong, *J. Am. Chem. Soc.*, 2011, **133**, 10878.

12- Y. Chen, L. Wang, G. (Max) Lu, X. Yao and L. Guo, *J. Mater. Chem.*, 2011, **21**, 5134.

13- J. Choi, S. Y. Ryu, W. Balcerski, T. K. Lee and M. R. Hoffmann, *J. Mater. Chem.*, 2008, **18**, 2371.

14- C. Xing, Y. Zhang, W. Yan and L. Guo, *Int. J. Hydrogen Energ.*, 2006, **31**, 2018.

15- S. Shen and L. Guo, *Mater. Res. Bull.*, 2008, **43**, 437.

16- X. Zong, H. Yan, G. Wu, G. Ma, F. Wen, L. Wang and C. Li, *J. Am. Chem. Soc.*, 2008, **130**, 7176.

17- X. Zong, G. Wu, H. Yan, G. Ma, J. Shi, F. Wen, L. Wang and C. Li, *J. Phys. Chem. C*, 2010, **114**, 1963.